

BULLETIN OF THE CHEMICAL SOCIETY OF JAPAN, VOL. 45, 720—725(1972)

## Excimer and Monomer Defect Emissions of Perylene and Pyrene Crystals as Studied by the Nanosecond Time-resolved Spectroscopy Technique

Akinori INOUE, Keitaro YOSHIHARA,\* Takahiro KASUYA,\* and Saburo NAGAKURA

*The Institute for Solid State Physics, The University of Tokyo, Roppongi, Minato, Tokyo**\*The Institute of Physical and Chemical Research, Wako, Saitama*

(Received September 21, 1971)

Nanosecond time-resolved fluorescence spectra were measured at 77°K for pyrene and perylene crystals, and anomalous emissions which have lifetimes of  $\sim 8$  nsec and are difficult to be found by the usual steady excitation, were observed at the higher-wave number sides of the usual excimer emissions. From the band position and the vibrational structure, the anomalous emission was interpreted as being due to monomer defects in each crystal. The analysis of the observed rise and decay curves of the monomer defect and excimer emissions shows that the excited states of both emissions are populated independently from the band level of each crystal excited by light irradiation. The temperature dependence of the emission indicates that a thermal activation of 0.035 eV is required for the excimer formation in a perylene single crystal, while no activation energy is required for the excitation of the monomer defect.

Excimer fluorescences from crystals of aromatic compounds were studied by various investigators<sup>1-5)</sup> and were found to be observed for only dimeric crystals, such as pyrene and perylene, in which the molecules exist in pairs.<sup>3)</sup> Birks, Kazzaz, and King<sup>5)</sup> observed the time dependence of the excimer fluorescence of the pyrene crystal. According to their findings, the excimer is formed at 293°K within one nanosecond after the excitation. Beside the excimer band, a partially-structured anomalous emission band was observed with the microcrystalline layer of pyrene.<sup>2,5)</sup> The band was assigned by Birks *et al.* to an emission from surface monomer defects excited by the encounter with excimer excitations.<sup>5)</sup>

An anomalous fluorescence band with a vibrational

structure was also observed by Tanaka for a single crystal of perylene at low temperatures below 50°K.<sup>4)</sup> This band is very similar in position and shape to the monomeric perylene band and was assigned to a monomer emission. Tanaka assumed that the excimer state was populated *via* an excited monomer state and estimated the potential barrier of the process to be 285 cm<sup>-1</sup> from an analysis of the observed temperature dependence of the excimer emission.<sup>4)</sup> According to this mechanism, the excimer emission may be expected to have a rise time which corresponds to the decay time of the monomer emission.

Under these circumstances, we have undertaken to study, by the nanosecond time-resolved spectroscopy technique, the rise and decay processes of fluorescent states of pyrene and perylene, in order to clarify the nature of the anomalous fluorescence and the energy-transfer mechanism in both dimeric crystals.

### Experimental

*Materials.* Pyrene was purified by zone refining after vacuum sublimation. Perylene was purified by the vacuum

- 
- 1) J. Ferguson, *J. Chem. Phys.*, **28**, 765 (1958).
  - 2) J. B. Birks and A. J. W. Cameron, *Proc. Roy. Soc.*, **249A**, 297 (1959).
  - 3) B. Stevens, *Spectrochim. Acta*, **18**, 439 (1962).
  - 4) J. Tanaka, *This Bulletin*, **36**, 1237 (1963).
  - 5) J. B. Birks, A. A. Kazzaz, and T. A. King, *Proc. Roy. Soc.*, **291A**, 556 (1966).

sublimation of a synthetic material.<sup>6)</sup> A single crystal of perylene was obtained by recrystallization from the toluene solution.

**Nitrogen Gas Laser.** A pulsed, coaxial-type nitrogen gas laser<sup>7,8)</sup> was built as an exciting source. The discharge voltage of the laser is about 30 kV, and the pressure of nitrogen is approximately 4 Torr. Coaxial transmission lines are used as a condenser for the discharge. The wavelength of the laser emission is 3371 Å, and the laser pulse has a duration of approximately 3 nanoseconds, with a peak power of about 20 kW. The repetition rate is 20 Hz, and the oscillatory behavior is quite regular.

**Fluorescence Measurements.** Fluorescence spectra were measured by means of a Bausch and Lomb monochromator, being detected by an RCA 1P28 photomultiplier. By means of the repetitive operation of the laser, the sampling technique was used to measure the time-resolved spectra, a Tektronix 3S1 sampling oscilloscope being used. By setting the delay of a Tektronix 3T77A sampling sweep unit at a fixed time, a time-resolved spectrum was obtained by scanning the wavelength and recording the average photocurrent. The spectral response of the photomultiplier was not calibrated.

The laser light was attenuated by filters in order to prevent the excitation-exciton interaction which causes a remarkable change in the decay characteristics of the fluorescences.<sup>9-11)</sup> A Toshiba UV-39 filter was set in front of the monochromator entrance slit in order to eliminate scattered laser light. For the purpose of analyzing the initial rise of emission, the exact pulse shape of the laser was measured by a Hamamatsu TV R317 biplanar photodiode and the sampling oscilloscope. The time resolution of the system was estimated to be about 0.5 nsec. A 3650 Å line from a high-pressure mercury lamp was used for the measurement of the fluorescence spectra by means of steady excitation.

## Results and Discussion

### Time-resolved Fluorescence Spectra and Lifetimes.

Nanosecond time-resolved fluorescence spectra were measured at 77°K for perylene and pyrene single crystals; the results are shown in Figs. 1 and 2, respectively. Fluorescence spectra observed by the steady-excitation technique for both crystals are also shown in these figures for purposes of comparison. Furthermore, the fluorescence lifetimes measured for both crystals at 293°K and 77°K are listed in Table 1. This table also includes the wave numbers of the observed fluorescence maxima. Two fluorescence spectra with different lifetimes were observed at 77°K for each crystal: one is at shorter wavelengths and is short-lived, while the other is at longer wavelengths and is long-lived.

By the steady-excitation technique, the short-lived emission is difficult to be observed distinctly for the

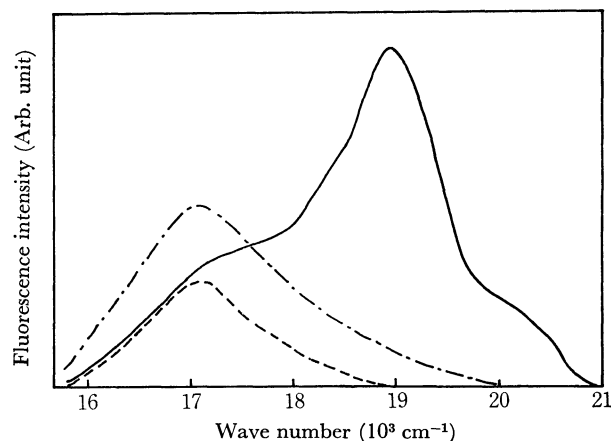


Fig. 1. Time-resolved fluorescence spectra of a perylene crystal at 77°K: —, 4 nsec after trigger; ----, 20 nsec after trigger; ····, fluorescence by steady excitation.

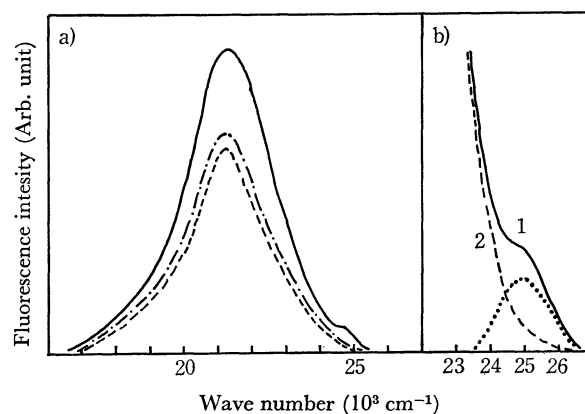


Fig. 2. a) Time-resolved fluorescence spectra of a pyrene crystal at 77°K: —, 4 nsec after trigger; ----, 10 nsec after trigger; ····, fluorescence by steady excitation. b) Time-resolved fluorescence spectra in the 25000 cm<sup>-1</sup> region observed with a pyrene crystal at 77°K, the emission higher than ~26000 cm<sup>-1</sup> being cut off by the used of a Toshiba UV-39 filter. The ordinate in b) is magnified compared with that in a): —, 4 nsec delay; ----, 10 nsec delay; ····, spectrum of the monomer defect fluorescence obtained by subtracting curve 2 from curve 1.

TABLE 1. FLUORESCENCE LIFETIMES ( $\tau$ ) AND MAXIMUM WAVE NUMBERS ( $\nu_{\max}$ ) OF PYRENE AND PERYLENE SINGLE CRYSTALS AT 293°K AND AT 77°K

	293°K		77°K	
	$\tau$ (ns)	$\nu_{\max}$ (cm <sup>-1</sup> )	$\tau$ (ns)	$\nu_{\max}$ (cm <sup>-1</sup> )
Pyrene	—	—	8	25300
	70	21500	180	21500
Perylene	—	—	8	19000
	44	17800	91	17000

single crystals in the temperature range from 77°K to 293°K. This is because it has a relatively low fluorescence quantum yield in this temperature range. By the nanosecond time-resolved spectroscopy technique, however, we can observe separately each of the short-lived and long-lived components of the emission spectrum. For example, the fluorescence spectrum of the perylene single crystal, observed 4 nsec after the trig-

6) The synthetic perylene was provided by Professor S. Iwashima, Meisei University and Professor H. Inokuchi, The University of Tokyo.

7) M. Geller, D. E. Altman, and T. A. DeTemple, *J. Appl. Phys.*, **37**, 3639 (1966).

8) A. Inoue, K. Yoshihara, S. Nagakura, T. Kasuya, A. Minoh, S. Kobayashi, and K. Shimoda, *Reports I.P.C.R.*, **47**, 40 (1971).

9) A. Bergman, M. Levine, and J. Jortner, *Phys. Rev. Lett.*, **18**, 593 (1967).

10) C. R. Goldschmidt, Y. Tomkiewicz, and I. B. Berlman, *Chem. Phys. Lett.*, **2**, 520 (1968).

11) A. Inoue, K. Yoshihara, and S. Nagakura, to be published.

ger pulse, has an intense structured band at  $\sim 19000 \text{ cm}^{-1}$  besides the band at  $\sim 17000 \text{ cm}^{-1}$  which still remains in the fluorescence spectrum observed 20 nsec after the trigger pulse. The long-lived components are identified with the excimer fluorescences for the following reasons: (1) the lifetime of the emission at longer wavelengths of the pyrene crystal at  $77^\circ\text{K}$ , 180 nsec, is very close to that of the excimer emission obtained by Birks, Kazzaz, and King<sup>5)</sup> (185 nsec); and (2) in both crystals, the time-resolved spectra of the long-lived emission coincide in their positions and shapes with the corresponding excimer fluorescence spectra obtained by the steady excitation.<sup>1-5)</sup> The short-lived fluorescence at  $\sim 19000 \text{ cm}^{-1}$  is very similar to that observed with the monomeric ( $\beta$ -type) perylene crystal and can safely be assigned to the excited monomer.<sup>4)</sup>

Concerning the pyrene single crystal, in addition to the excimer fluorescence at  $21500 \text{ cm}^{-1}$ , the short-lived emission was observed at  $25300 \text{ cm}^{-1}$  in the spectrum 10 nsec after the trigger pulse. The latter is similar to the spectrum due to the monomer defect observed by Birks *et al.*<sup>2,5)</sup> with a very thin film of pyrene.

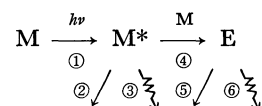
The emissions at shorter wavelengths observed for both single crystals are anomalous in the sense that they are distinctly observed only by the nanosecond time-resolved spectroscopy technique at  $77^\circ\text{K}$ . On the other hand, when thin evaporated films are used instead of the single crystal, the anomalous emission can be observed by the steady-excitation technique for both aromatic hydrocarbons, even at room temperatures.

*Examination of the Previous Mechanisms of the Anomalous Emissions.* The two mechanisms were presented previously by Birks *et al.* and by Tanaka for the anomalous emissions observed for the pyrene and perylene crystals, respectively.

First, let us consider the mechanism presented by Birks *et al.*<sup>5)</sup> If the anomalous emission of the pyrene crystal is assumed to originate from excited surface monomer defects which are populated by the encounter

with excimer excitons,<sup>5)</sup> the anomalous fluorescence should have a rise time comparable to the decay time of the excimer exciton. The time dependence of the anomalous emission observed with pyrene crystals at  $25000 \text{ cm}^{-1}$  at  $77^\circ\text{K}$  is shown in Fig. 3. The rise time of the anomalous fluorescence is very short compared with the decay time of the excimer fluorescence. This clearly contradicts the mechanism presented by Birks *et al.*

We will check, from the kinetic point of view, the mechanism presented by Tanaka, which is schematically shown as follows:



Here, processes ①, ②, ③, ④, ⑤, and ⑥ are respectively concerned with the excitation of the monomer M, the radiative and radiationless decay processes of the excited monomer, M\*, the excimer formation process, and the radiative and radiationless decay processes of the excimer, E. According to this mechanism, the exciton concentrations of the monomer and excimer under pulse excitation may be represented as follows:

$$d[\text{M}^*]/dt = I(t) - (k_2 + k_3 + k_4[\text{M}])[\text{M}^*] \quad (1)$$

$$d[\text{E}]/dt = k_4[\text{M}^*][\text{M}] - (k_5 + k_6)[\text{E}] \quad (2)$$

Here,  $[\text{M}^*]$ ,  $[\text{E}]$ , and  $[\text{M}]$  represent the concentrations of the corresponding specimens,  $k_n$  is the rate constant for the above-mentioned process  $n$ , and  $I(t)$  is the rate of the generation of singlet monomer excitons, which may be expected to be proportional to the intensity of an incident light pulse. Equations (1) and (2) can be solved as follows:

$$[\text{M}^*] = \exp(-t/\tau_{\text{M}}) \int_0^t \exp(\xi/\tau_{\text{M}}) I(\xi) d\xi \quad (3)$$

$$[\text{E}] = \exp(-t/\tau_{\text{E}}) \int_0^t \exp((1/\tau_{\text{E}} - 1/\tau_{\text{M}})\xi) d\xi \times \int_0^\xi \exp(\eta/\tau_{\text{M}}) I(\eta) d\eta \quad (4)$$

Here,  $\tau_{\text{M}}$  and  $\tau_{\text{E}}$  are the lifetimes of the monomer and excimer defined as  $1/\tau_{\text{M}} = k_2 + k_3 + k_4[\text{M}]$  and  $1/\tau_{\text{E}} = k_5 + k_6$ , respectively. The monomer and excimer fluorescences are proportional to the concentrations of the monomer and excimer excitons, respectively. The equations were numerically integrated using the experimentally-determined shape of  $I(t)$  and the measured lifetimes shown in Table 1. It is necessary to consider the distortion in the observed fluorescence time-dependence curve due to the inability of the measuring circuit to follow an extremely fast rise. The actual method for correcting the distortion by the aid of a simple theory of the four-terminal network will be described in the Appendix. The time dependence of the excimer fluorescence was evaluated by applying Eq. (4) to the perylene crystal at  $77^\circ\text{K}$ ; the result is shown by a broken line in Fig. 4. In this figure, the observed result is also shown by open circles for the purpose of comparison. A marked discrepancy exists between the calculated and experimental results. A similar discrepancy was also found for the pyrene crystal, as clearly seen in Fig. 3.

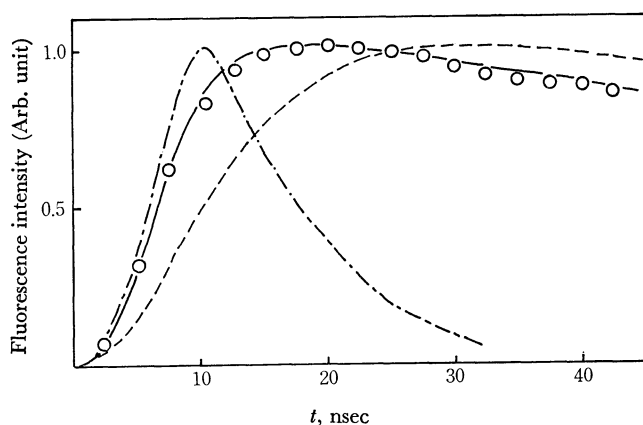


Fig. 3. Time dependence of the fluorescence of a pyrene crystal:—, calculated for the excimer fluorescence based on the present mechanism;---, calculated for the excimer fluorescence based on the mechanism presented by Tanaka; ····, observed curve for the monomer defect fluorescence; —○— observed points for the excimer fluorescence at  $77^\circ\text{K}$ .

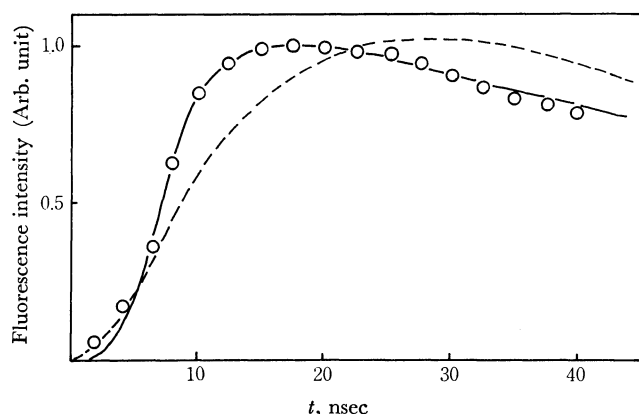


Fig. 4. Time dependence of the excimer fluorescence of a perylene crystal:—, calculated based on the present mechanism;---, calculated based on the mechanism presented by Tanaka; —○—, observed points at 77°K.

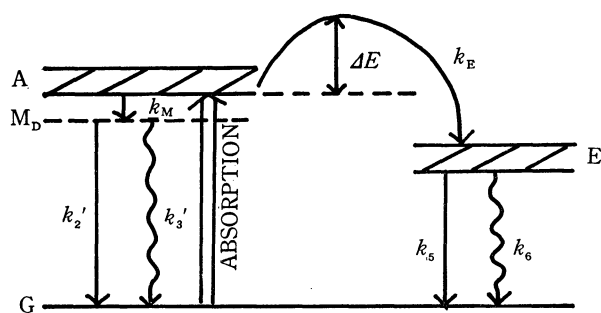


Fig. 5. Schematic diagram representing the mechanism of the excimer and the defect fluorescence of perylene and pyrene crystals.

It is obvious that neither of the two mechanisms presented previously can explain the rise and decay processes of the emissions of pyrene and perylene crystals.

*A New Mechanism for the Excimer and Anomalous Emissions.*

Here, we propose a new mechanism for the appearance of the monomer defect and excimer fluorescences. (see Fig. 5). Crystals are excited to a band whose excitation energy corresponds to the photon energy of 29700  $\text{cm}^{-1}$  of the nitrogen gas laser. After the excitation, a slight change in the orientation of paired molecules may take place in the formation of the excimer fluorescent state. The rate constant,  $k_E$ , for this process can be represented by  $k_E = k_{E0} \exp(-\Delta E/kT)$ , where  $\Delta E$  is a potential barrier for this process and where  $k_{E0}$  is a temperature-independent constant. A relaxation to the monomer-defect states also takes place from the excited band level with the rate constant  $k_M$ , which has been experimentally determined to be temperature-independent. Actual dimeric crystals contains a number of defect sites occupied by "unpaired" molecules, particularly at the crystal surface. In the perylene crystal, the most intense component around 19000  $\text{cm}^{-1}$  of the defect emission corresponds to the 0—1 band of the perylene-monomer emission, while the 0—0 band appears near 20000  $\text{cm}^{-1}$ <sup>12)</sup> and its intensity is considerably reduced by reabsorption.

12) K. Kawaoka and D. R. Kearns, *J. Chem. Phys.*, **45**, 147 (1966).

The following rate equations are obtained according to the new mechanism:

$$d\rho/dt = I(t) - (k_M + k_E)\rho \quad (5)$$

$$d[M_D]/dt = k_M\rho - (k_2' + k_3')[M_D] \quad (6)$$

$$d[E]/dt = k_E\rho - (k_5 + k_6)[E] \quad (7)$$

Here,  $\rho$  is the exciton population in the excited band level, and the population of the monomer defect is represented by  $[M_D]$ . The rate constants  $k_2'$  and  $k_3'$  stand for those of the radiative and radiationless deactivations of the defect state, respectively, while  $k_5$  and  $k_6$  stand for those of the excimer state. Since  $k_M$  and  $k_E$  are much larger than  $k_2'$ ,  $k_3'$ ,  $k_5$ , and  $k_6$ , the stationary state condition may safely be applied to Eq. (5). Thus, the two concentrations  $[M_D]$  and  $[E]$  can be expressed as:

$$[M_D] = k_M/(k_M + k_E) \exp(-t/\tau_M) \int_0^t \exp(\xi/\tau_M) I(\xi) d\xi \quad (8)$$

and

$$[E] = k_E/(k_M + k_E) \exp(-t/\tau_E) \int_0^t \exp(\xi/\tau_E) I(\xi) d\xi \quad (9)$$

Here,  $\tau_M$  and  $\tau_E$  are the lifetimes of the defect and excimer emissions, defined as  $1/\tau_M = k_2' + k_3'$  and  $1/\tau_E = k_5 + k_6$ . The rise curve of the excimer fluorescence was obtained by the numerical integration of Eq. (9) using the measured lifetime and the shape of the laser pulse. The curve obtained for the perylene crystal at 77°K is shown by a solid line in Fig. 4; it is in good agreement with the experimental results. The same mechanism was also applied to the pyrene crystal, with a good agreement between the calculated and observed rise curves, as is shown in Fig. 3. These results show that, in both crystals, the excimer excitons are not produced *via* the excited monomer; rather, both excited states are populated independently from the band levels of the crystals excited by the light irradiation.

*Temperature Dependence of Emissions.* According to our new mechanism, the intensity ratio of the excimer fluorescence to the anomalous fluorescence obtained by the steady excitation,  $I_E/I_M$ , can be written as:

$$I_E/I_M = k_E k_5 (k_2' + k_3') / k_M k_2' (k_5 + k_6) \quad (10)$$

The experimental value,  $\tau_E^{-1}$ , can be expressed<sup>5)</sup> by the sum of the temperature-dependent and temperature-independent rate constants:

$$\tau_E^{-1} = k_5 + k_6 = k_5^0 + k_6^0 \exp(-\Delta W/kT) \quad (11)$$

where  $k_5^0$ ,  $k_6^0$ , and  $\Delta W$  are the frequency factor, the temperature-independent rate constant, and the activation energy. The plots of  $\ln(\tau_E^{-1} - k_5^0 - k_6^0)$  versus  $1/T$  give a linear relation, as shown in Fig. 6, with  $k_5 + k_6 = 1.2 \times 10^7 \text{ sec}^{-1}$  and  $\Delta W = 680 \text{ cm}^{-1}$  for the perylene crystal. This may be compared with the value of  $\Delta W = 530 \text{ cm}^{-1}$  for the pyrene crystal given by Birks, Kazzaz, and King.<sup>5)</sup> The results show that the exponential term may be disregarded in the temperature range below 100°K and that, therefore,  $k_5 + k_6$  may be regarded as temperature independent in this temperature range. Furthermore, the present experiment shows that the lifetime of the monomer-defect emission is temperature independent between 77—135°K within the limits of experimental error. Since the radiative

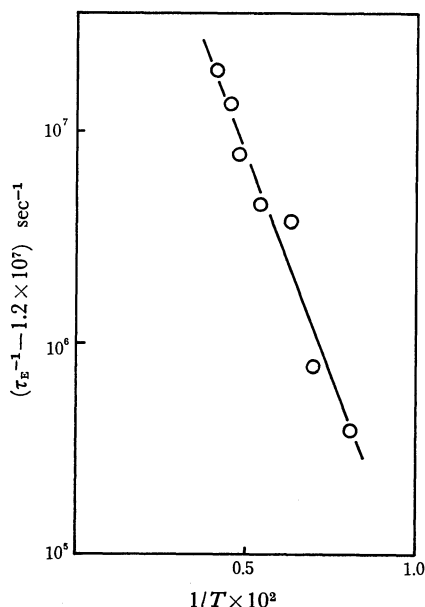


Fig. 6. Temperature dependence of the excimer fluorescence lifetime of a perylene crystal. Semilogarithmic plots of  $(\tau_E^{-1} - 1.2 \times 10^7)$  versus  $1/T$ .

rate constants may reasonably be assumed to be temperature independent, the temperature dependence of  $I_E/I_M$  given by Eq. (10) actually shows that of  $k_E/k_M$ .

To elucidate the natures of  $k_M$  and  $k_E$ , the temperature dependences of  $k_E/(k_M + k_E)$  and  $k_M/(k_M + k_E)$  were measured for the perylene crystal between 92–220°K and between 83–135°K, respectively. These values can be obtained by measuring the fluorescence intensity divided by the lifetime, *i.e.*,

$$\begin{aligned} I_E/\tau_E &= C_1(k_E/(k_M + k_E))(k_5/(k_5 + k_6))(k_5 + k_6) \\ &= C_1 k_E k_5 / (k_M + k_E) \end{aligned} \quad (12)$$

In a similar way,

$$I_M/\tau_M = C_2 k_M k_2' / (k_M + k_E) \quad (13)$$

Here,  $C_1$  and  $C_2$  are temperature-independent constants. The fluorescence intensities,  $I_E$  and  $I_M$ , can be written as follows:

$$I_E = \int d\nu \int_0^\infty F_{E\nu}(t) dt \quad I_M = \int d\nu \int_0^\infty F_{M\nu}(t) dt \quad (14)$$

where  $F_{E\nu}(t)$  and  $F_{M\nu}(t)$  are the time dependences of the excimer and monomer-defect fluorescences at a wave number,  $\nu$ . The integrals for  $I_E$  and  $I_M$  with respect to the wave number are performed over the excimer- and defect-emission bands, respectively.

Setting  $F_{E\nu}(t) = F_{E\nu}^0 \exp(-(t_0 - t)/\tau_E)$  and  $F_{M\nu}(t) = F_{M\nu}^0 \exp(-(t_0 - t)/\tau_M)$ , where  $F_{E\nu}^0$  and  $F_{M\nu}^0$  are the fluorescence intensities at  $t = t_0$ , we can obtain:

$$I_E/\tau_E = \exp(t_0/\tau_E) \int F_{E\nu}^0 d\nu \quad I_M/\tau_M = \exp(t_0/\tau_M) \int F_{M\nu}^0 d\nu \quad (15)$$

Therefore, the temperature dependence of  $k_E/(k_M + k_E)$  was obtained by integrating each of the time-resolved spectra (at a fixed time,  $t_0$ ) of the excimer observed at several different temperatures and by being multiplied by  $\exp(t_0/\tau_E)$ . Since, according to our experiment, the monomer-defect emission exhibits no change in its position and shape in the temperature range of 77–

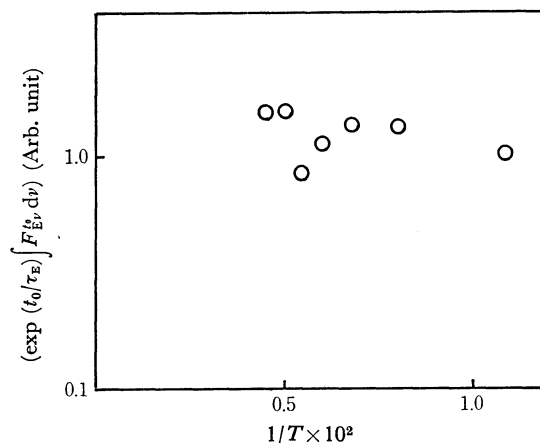


Fig. 7. Temperature dependence of the excimer fluorescence intensity of a perylene crystal obtained by the integration of time-resolved spectra at 20 nsec delay. Semilogarithmic plots of  $(\exp(t_0/\tau_E) \int F_{E\nu}^0 d\nu)$ ,  $t_0 = 20$  nsec versus  $1/T$ .

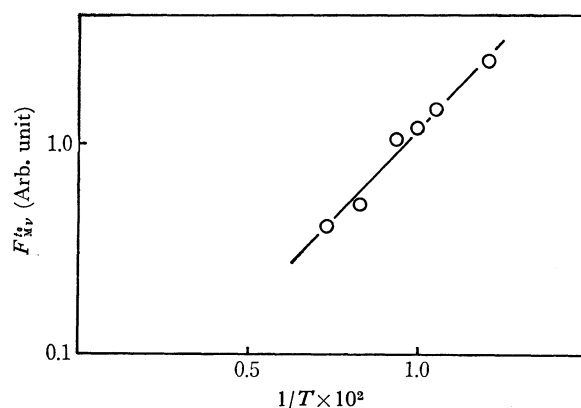


Fig. 8. Temperature dependence of the peak intensity of the defect fluorescence of a perylene crystal. Semilogarithmic plots of  $F_{M\nu}^0$ ,  $t_0 = 4$  nsec versus  $1/T$ .

135°K, the temperature dependence of  $k_M/(k_M + k_E)$  was measured by observing the emission intensity 4 nsec after a trigger pulse at 19000  $\text{cm}^{-1}$ . The results are shown in Figs. 7 and 8. The plots of  $\ln(k_M/(k_M + k_E))$  versus  $1/T$  in the temperature range of 96–135°K give a straight line, with an activation energy of  $\Delta E = 280 \text{ cm}^{-1}$ . On the other hand,  $k_E/(k_M + k_E)$  is almost independent of the temperature within the range of 92–220°K. This directly indicates the inequality relation  $k_E \gg k_M$  in this temperature range. The temperature dependences of  $k_M/(k_M + k_E)$  and  $k_E/(k_M + k_E)$  show that the monomer defect emission is intense at lower temperatures, while the excimer emission is almost constant at the temperatures above 90°K. This is in good agreement with the results obtained by the steady-excitation experiment. The results are also consistent with the fact that the quantum yield of the monomer defect emission is relatively small.

The activation energy thus obtained is in agreement with that obtained previously by the steady-excitation experiment,<sup>4)</sup> but the mechanism of energy transfer should be reinterpreted according to the present mechanism.

*Emissions from the Thin Films of Perylene and Pyrene.* In a thin evaporated film which has a much higher concentration of the monomer defect relative to the regular site than a single crystal, the defect emission may be expected to be observed easily by the steady excitation at as high a temperature as 77°K. This is actually the case for a perylene evaporated film (thickness  $\sim 0.3 \mu\text{m}$ ), and its peak intensity at  $19000 \text{ cm}^{-1}$  is comparable with the excimer fluorescence intensity at 77°K. The monomer-defect emission was also observed for a pyrene-evaporated layer.<sup>2,5)</sup>

We wish to express our thanks to Dr. M. Geller of the U.S. Naval Electronics Laboratory Center for his kind suggestions about making a coaxial transmission line nitrogen gas laser. We are also greatly indebted to Professor S. Iwashima, Meisei University, and Professor H. Inokuchi, The University of Tokyo, for their kindness in providing us with synthetic materials. Our thanks are also due to Dr. M. Takami, The Institute of Physical and Chemical Research, and Mr. T. Kobayashi for their helpful discussions.

### Appendix

The correction for the measured time dependence of the fluorescence was made as follows. An integration circuit assumed for the detector system including the photomultiplier and the oscilloscope, consists of a resistor,  $R$ , and a capacitor,  $C$ , as shown schematically in Fig. 9. From the theory of the four-terminal network, the ratio of the Fourier-transformed output signal,  $G(\omega)$ , to the input signal,  $F(\omega)$ , is given by:

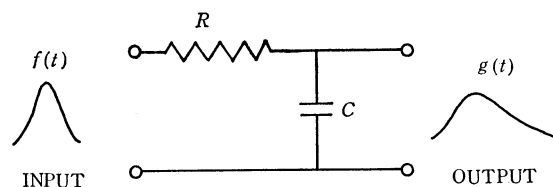


Fig. 9. A model circuit containing a resistor  $R$  and a capacitor  $C$  of the measuring system.

$$G(\omega)/F(\omega) = 1/(1 + i\omega CR) \quad (\text{A1})$$

where

$$F(\omega) = \int_0^{\infty} dt \exp(-i\omega t) f(t),$$

$$G(\omega) = \int_0^{\infty} dt \exp(-i\omega t) g(t), \quad (\text{A2})$$

and  $f(t)$  and  $g(t)$  are the time dependences of the input and output signals, respectively. The output signal,  $g(t)$ , is obtained by an inverse transformation of  $G(\omega)$  and by the aid of the equation (A1):

$$g(t) = (1/CR) \exp(-t/CR) \int_0^t f(\xi) \exp(\xi/CR) d\xi \quad (\text{A3})$$

By the aid of Eq. (A3), the time constant,  $CR$ , can be determined in such a way that the integration of the experimentally-determined  $f(t)$  fits into  $g(t)$  as well as possible. Both  $f(t)$  and  $g(t)$  were obtained by observing the same laser pulse by a fast photodiode and a 1 GHz sampling oscilloscope, and by a photomultiplier and an 80 MHz oscilloscope, respectively. The actual integration of  $f(t)$  fits well into  $g(t)$  over a wide range of  $t$  with  $CR = 3.5 \text{ nsec}$ , suggesting that the original assumption is correct.